arXiv:cond-mat/0301546v1 [cond-mat.str-el] 28 Jan 2003

Longitudinal magnon in the tetrahedral spin system $Cu_2Te_2O_5Br_2$ near quantum criticality

C. Gros[1], P. Lemmens[2,4], M. Vojta[3], R. Valentí[1], K.-Y. Choi[4], H. Kageyama[5], Z. Hiroi[5], N.V. Mushnikov[5], T. Goto[5] M. Johnsson[6], P. Millet[7]

[1] *Fakultät 7, Theoretische Physik, Universität des Saarlands, D-66041 Saarbrücken, Germany.*
[2] *Max Planck Institute for Solid State Research, D-70569 Stuttgart, Germany*
[3] *Theoretische Physik III, Universität Augsburg, D-86135 Augsburg, Germany*
[4] *2. Physikalisches Institut, RWTH Aachen, D-52056 Aachen, Germany*
[5] *Institute for Solid State Physics, Univ. of Tokyo Kashiwa-shi, Chiba 277-8581, Kashiwa, Japan*
[6] *Department of Inorganic Chemistry, Stockholm Univ., S-10691 Stockholm, Sweden*
[7] *Centre d'Elaboration de Matériaux et d'Etudes Structurales, CEMES/CNRS, F-31062 Toulouse, France*

We present a comprehensive study of the coupled tetrahedra-compound $Cu_2Te_2O_5Br_2$ by theory and experiments in external magnetic fields. We report the observation of a longitudinal magnon in Raman scattering in the ordered state close to quantum criticality. We show that the excited tetrahedral-singlet sets the energy scale for the magnetic ordering temperature T_N. This energy is determined experimentally. The ordering temperature T_N has an inverse-log dependence on the coupling parameters near quantum criticality.

PACS numbers: 75.30.Gw, 75.10.Jm, 78.30.-j

Introduction.- Quantum fluctuations in antiferromagnetic insulators lead to a reduction of the magnetic moment and to a new mode in which the magnitude of the local order parameter oscillates, the longitudinal magnon (LM) [1] (see Fig. 1(a)). This elementary excitation is absent in classical magnets, where the excitations perform a precession of the moment around its equilibrium position and are therefore transversaly polarized (see Fig. 1(b)). The longitudinal mode is difficult to observe since it occurs only in quantum spin systems with reduced dimensionality. Only recently a LM has been detected by inelastic neutron scattering in quantum spin-$\frac{1}{2}$ [2,3] and spin-1 [4,5] chain compounds.

Quantum spin-fluctuations are of special importance in quasi-zero dimensional systems with weakly coupled spin clusters. These lattices allow for quantum phase transitions between magnetically ordered states and non-magnetic phases with a spin gap. The recently discovered [6] spin-tetrahedral compounds $Cu_2Te_2O_5X_2$ (X=Cl, Br) have been shown to order at transition temperatures $T_N^{(Cl)} = 18.2$ K and $T_N^{(Br)} = 11.4$ K which are strongly suppressed with respect to the magnitude of the intra-tetrahedral couplings [7]. Unconventional Raman-scattering has been found in the magnetic channel [7,8] and the occurrence of low-lying singlet excitations has been proposed [6]. Plateaus in the magnetization have been predicted for a related linear chain of spin tetrahedra [9].

The nature of the ordered states in $Cu_2Te_2O_5X_2$ has not yet been settled. The ordering temperature $T_N^{(Cl)}$ and $T_N^{(Br)}$ decreases and rises respectively with an external magnetic field [7]. This unusual magnetic field-induced stabilization of $T_N^{(Br)}$ motivated in part the present study. A decrease of T_N is typical for an antiferromagnet in the classical limit. We will show later on that T_N may rise near a quantum-phase transition. This results then indicates $Cu_2Te_2O_5Br_2$ to be close to criticality.

Here we report the observation of a LM in $Cu_2Te_2O_5Br_2$ by Raman scattering in a magnetic field and present the evolution of this mode under the influence of an external magnetic field. We believe that

this study constitutes the first time that a longitudinal magnon is detected optically as well as the first observation of such a mode in a tetrahedral spin system, i.e. in a system with an even number of spins per unit cell. Furthermore, high-field magnetization and other thermodynamic data on pure and substituted $Cu_2Te_2O_5(Br_xCl_{1-x})_2$ are compared via a mean-field analysis which allows to determine the microscopic parameters for $Cu_2Te_2O_5Br_2$. We find, interestingly, that the scale of the ordering temperature T_N is set by the (non-magnetic) excited singlet of the copper tetrahedron and that T_N has an essential singularity at criticality.

Mean-field approach.- We assume that the basic spin-cluster in this compound is given by the copper tetrahedron (see inset in Fig. (2)). We denote with s_{kl} the spin-singlet state of two intra-tetrahedral sites k and l and with t^α_{kl} the respective triplet states, with $\alpha = \pm 1, 0$. We start by considering the eigenstates of the isolated tetrahedra with $H_t = J_1[(\mathbf{S}_1 + \mathbf{S}_2)\cdot(\mathbf{S}_3 + \mathbf{S}_4)] + J_2(\mathbf{S}_1 \cdot \mathbf{S}_2 + \mathbf{S}_3 \cdot \mathbf{S}_4)$, which consist of two singlets, three triplets and one quintuplet.

For $J_2 < J_1$ the ground state singlet ψ_{s1} and the excited singlet ψ_{s2} are

$$\psi_{s1} = \frac{-1}{\sqrt{3}}\left[t^0_{12}t^0_{34} - t^+_{12}t^-_{34} - t^-_{12}t^+_{34}\right] \ , \qquad \psi_{s2} = s_{12}s_{34} \tag{1}$$

with eigenenergies $E_{s1} = -2J_1 + J_2/2$ and $E_{s2} = -3J_2/2 = E_{s1} + \Delta E_{s2}$, with $\Delta E_{s2} = 2J_1 - 2J_2$. The three triplets ψ^α_{t1}, ψ^α_{t2} and ψ^α_{t3} have the (excitation) energies $\Delta E_{t1} = J_1$, $\Delta E_{t2} = \Delta E_{t3} = 2J_1 - J_2$ with respective eigenstates

$$\begin{aligned} \psi^0_{t1} &= \frac{1}{\sqrt{2}}(t^+_{12}t^-_{34} - t^-_{12}t^+_{34}), \\ \psi^-_{t1} &= \frac{1}{\sqrt{2}}(t^0_{12}t^-_{34} - t^-_{12}t^0_{34}) \\ \psi^+_{t1} &= \frac{1}{\sqrt{2}}(t^+_{12}t^0_{34} - t^0_{12}t^+_{34}) \\ \psi^\alpha_{t2} = s_{12}t^\alpha_{34}, &\qquad \psi^\alpha_{t3} = t^\alpha_{12}s_{34} \end{aligned} \tag{2}$$

The quintuplet has the energy $\Delta E_q = 3J_1$. The inter-tetrahedra couplings can be described in a mean-field approach by [10]:

$$H_{MF} = -J_c M\left(S^z_1 + S^z_2 - S^z_3 - S^z_4\right) \ , \quad \text{and} \quad M = \frac{1}{4}\langle S^z_1 + S^z_2 - S^z_3 - S^z_4\rangle \tag{3}$$

with M being the staggered magnetization order parameter. J_c is here the sum over all inter-tetrahedra couplings.

The mean-field Hamiltonian H_{MF} couples ψ_{s1} and ψ^0_{t1} leading to new eigenstates for $H = H_t + H_{MF}$:

$$\begin{aligned} |\varphi\rangle &= \cos\varphi\,|\psi_{s1}\rangle + \sin\varphi\,|\psi^0_{t1}\rangle, \\ |\tilde{\varphi}\rangle &= \sin\varphi\,|\psi_{s1}\rangle - \cos\varphi\,|\psi^0_{t1}\rangle \end{aligned} \tag{4}$$

with $\langle\tilde{\varphi}|\varphi\rangle = 0$ and new energies

$$\Delta E_{\varphi,\tilde{\varphi}} = \frac{J_1}{2}\left[1 \mp \sqrt{1 + 32M^2J_c^2/(3J_1^2)}\right] \tag{5}$$

with $\tan\varphi = -\Delta E_\varphi\sqrt{6}/(4J_cM)$. $|\varphi\rangle$ is the ground-state and $|\tilde{\varphi}\rangle$ can be identified as a longitudinal magnon excitation. The physical interpretation of this excitation is as follows. When J_c=0 we have isolated tetrahedra and $|\tilde{\varphi}\rangle$ would correspond to the excited intra-tetrahedral triplet state $|\psi^0_{t1}\rangle$. For $J_c \neq 0$, $|\tilde{\varphi}\rangle$ evolves continuously from ψ_{t_1} as a function of the inter-tetrahedral coupling J_c and becomes soft at the transition-point to the ordered state. The molecular field couples also ψ_{t1} with the quintuplet ψ_q, though we neglect this coupling here since we are interested in phases with low transition temperatures T_N for which the high-energy quintuplet does not contribute significantly.

The calculation of the staggered magnetization $M = Tr[(S^z_1 + S^z_2 - S^z_3 - S^z_4)\mathrm{e}^{-\beta H}]/(4Z)$ (Eq. 3) leads to the following self-consistency equation,

$$M = \frac{\mathrm{e}^{-\beta E_\varphi} - \mathrm{e}^{-\beta E_{\tilde{\varphi}}}}{Z}\sqrt{\frac{2}{3}}\frac{\tan\varphi}{1+\tan^2\varphi} \ , \tag{6}$$

where $\beta = 1/T$ and Z is the partition function for the coupled tetrahedra system, i.e. $Z = \mathrm{e}^{-\beta E_{s1}} + \mathrm{e}^{-\beta E_{s2}} + \ldots$. For $J_c = J_c^{(qc)} = 3J_1/4$ the magnetization M goes to zero and the system shows a second-order phase transition at T_N.

Results.- The transition-temperature T_N can be obtained from (6) by imposing $M = 0$. Assuming that (i) s_2 is the lowest excited state of a tetrahedron and (ii) at small temperatures only the leading order in a $1/T$ expansion is contributing in Eq. (6), T_N can be analytically derived:

$$T_N \simeq \Delta E_{s2}\ \log^{-1}\left(J_c^{(qc)}/(J_c - J_c^{(qc)})\right) \ , \tag{7}$$

T_N shows an inverse-log singularity close to the quantum critical point at $J_c = J_c^{(qc)}$. The critical $J_c^{(qc)} = 3J_1/4$ is independent of J_2. In Fig. (2) we plot T_N as a function of J_c both as obtained in the analytic solution Eq. (7) and by solving numerically the self-consistent equation Eq. 6. Note that for the region $J_c \sim J_c^{(qc)}$, Eq. (7) provides a good approximation for T_N.

The inverse-log dependence of the Neél-temperature implies that T_N is substantial even near the quantum critical point, as illustrated in Fig. (2), in contrast to the magnitude of the zero-temperature magnetic moment,

$$M(T=0) = \frac{1}{\sqrt{6}}\sqrt{1 - \left(J_c^{(qc)}/J_c\right)^2} \ , \tag{8}$$

which has a standard mean-field form [11] (compare Fig. (2)). For $J_2 > J_1$ the tetrahedral ground-state changes

to ψ_{s_2} and the non-magnetic singlet ψ_{s_2} sets therefore the scale for T_N.

States in an external field.- An external longitudinal magnetic field does not induce additional couplings in between the different eigenstates but it leads to shifts in the respective eigenenergies. A transversal magnetic field B_x induces, on the other hand, a coupling in between ψ^0_{t1} and $\psi^{\pm}_{t1}$ (see Eq. (2)). The mean-field ground state, which breaks rotational invariance, can be written, in lowest order in B_x, as

$$|\varphi, B_x\rangle = \cos\alpha\,|\varphi\rangle + \frac{\sin\alpha}{\sqrt{2}}\Big[|\psi^+_{t1}\rangle + |\psi^-_{t1}\rangle\Big], \qquad (9)$$

with $\tan\alpha = B_x \sin\varphi/(J_1 - \Delta E_\varphi)$. In lowest order in B_x, the ground-state energy, $\Delta E_{\varphi,B_x} = E_{\varphi,B_x} - E_\varphi$,

$$\Delta E_{\varphi,B_x} = -B_x^2 \sin^2\varphi/(J_1 - \Delta E_\varphi), \qquad (10)$$

decreases quadratically with B_x.

This result has an interesting consequence for the transition temperature. The energy of the excited singlet E_{s2} is not affected by B_x, its relative energy to the ground state ΔE_{s2} increases consequently with B_x (compare Eq. (10)). Eq. (7) tells us then that the Néel temperature also increases with B_x [13]. An order-of magnitude estimate of the effect for $Cu_2Te_2O_5Br_2$ and $B_x = 13\,\mathrm{T}$ yields $\Delta T_N \approx 0.8\,\mathrm{K} = 0.56\,\mathrm{cm}^{-1}$ which agrees well with the experimentally observed raise of $\sim 1\,\mathrm{K}$ reported already in Ref. [7].

For the longitudinal magnon, a calculation analogous to Eq. (10) leads to

$$\Delta E_{\tilde\varphi,B_x} = -B_x^2 \cos^2\varphi/(J_1 - \Delta E_{\tilde\varphi}), \qquad (11)$$

The resulting change $\Delta E_{\tilde\varphi,B_x} = E_{\tilde\varphi,B_x} - E_{\tilde\varphi}$ in the longitudinal-magnon energy is positive, as $J_1 - \Delta E_{\tilde\varphi} < 0$, and substantially larger than the shift for the ground-state $\Delta E_{\varphi,B_x}$ (and correpondingly for E_{s2}) since $\cos^2\varphi \gg \sin^2\varphi$. As we shall discuss in the next sections, this trend is qualitatively in agreement with the Raman data presented below.

Substitution experiments.- Specific heat and high-field magnetization have been measured on $Cu_2Te_2O_5(Br_xCl_{1-x})_2$ powder samples with $x = 1, 0.75, 0.66$ and 0.0 [6,7]. Substituting Br by Cl leads to a continuous decrease of the unit cell volume by 7% (x=0) and an increase of the transition temperature from 11.4 to 18.2 K. Also other physical properties change continuously with substitution [12]. In our coupled-cluster model we expect that the decrease of the unit cell volume is described by an increase of the coupling constant J_c. We have calculated the specific heat

$$C_v = \beta^2\langle(H - \langle H\rangle)^2\rangle \qquad (12)$$

in the mean-field approximation. In Fig. 3 the results are shown for various J_c values. In the inset of Fig. 3 the evolution of the experimentally determined specific heat as a function of substitution x is presented. Note that the mean-field results for increasing J_c reproduce the continuous shift of the specific heat anomaly to higher temperatures wit decreasing x.

A further support to the interpretation of these systems as that of coupled tetrahedra with a mean-field J_c inter-tetrahedra coupling and with a T_N ordering temperature, is obtained from high-field magnetization measurements which are presented in Fig. 4. We observe a finite slope for all samples at small fields which increases with decreasing x. Extrapolating M(H) from high to low fields a finite crossover field, H_{cross}= 12 T, 5 T and $\approx$ 0 T respectively, is defined as a function of decreasing x. No direct evidence for a plateau in the magnetization is found. A plateau at M=1/2 is predicted for a 1D chain of spin tetrahedra with parameters placing the system in the gapped phase [9], what leads us to conclude that these systems cannot be described as chains of tetrahedra. The finite slope in M(H) at small fields and even for x=1 is intrinsic and points to the underlying weak Néel state. The corresponding anisotropy is observed in single crystal susceptibility shown in the inset of Fig. 4. The transition is evident as a kink in χ(T) with a magnetic field perpendicular to the c-axis.

Raman spectroscopy.- We have performed Raman scattering experiments on c-axis oriented single crystals with diameters Ø $\approx$ 0.2 mm and length l $\approx$ 1 mm. The used scattering geometry in (cc) light scattering polarizations corresponds to **A** symmetry [7]. The magnetic field has been applied perpendicular to the light scattering polarization. In Fig. (5) we present Raman data for $Cu_2Te_2O_5Br_2$ in magnetic fields up to 6 T. We observe a shift of the low-energy magnetic mode at $\nu_{long} = 16.3\,\mathrm{cm}^{-1} = 23.4\,\mathrm{K}$ (for $B = 0$) to higher energies as a function of B and the appearance of an additional, magnetic field-induced mode at $\nu_{sing} = 23.2\,\mathrm{cm}^{-1} = 33.2\,\mathrm{K}$ ($B \neq 0$). In the inset Fig. (5a) the low energy spectrum is displayed with smaller optical slit width and higher spectral resolution. The intensity of the higher energy mode increases with field. It is not observable for $B = 0$.

In Fig. (5b) the energies of the respective modes are shown as a function of the magnetic field. While the higher energy mode does not show an appreciable magnetic field dependence (upper open symbols), the lower energy mode shows a nonlinear dependence on the magnetic field (lower full and open symbols). The full line in Fig. (5b) is a fit to the data proportional to the square of the magnetic field. The dashed curve describing the higher energy mode is proportional to the weaker, positive field dependence of the transition temperature as determined by specific heat and magnetic susceptibility measurements [7]. In the following we shall argue that these two modes at $\nu_{long} = 16.3\,\mathrm{cm}^{-1}$ and at $\nu_{sing} = 23.2\,\mathrm{cm}^{-1}$ can be identified as a longitudinal magnon mode and as an excitation to the second singlet

ψ_{s2} in Eq. (1) respectively.

Excited singlet.- We interpret the additional higher energy mode at $\nu_{sing} = 23.2\,\mathrm{cm}^{-1}$ presented in Fig. (5) as a transition to the second singlet $\psi_{s2} = s_{12}s_{34}$. Since this system is noncentrosymmetric, there is a nonzero Dzyaloshinski-Moriya (DM) [14] interaction. Assuming a DM contribution to the Raman operator, i.e. $H_R^{(DM)} \sim \mathbf{D}_{ij} \cdot (\mathbf{S}_i \times \mathbf{S_j})$ we find a non-zero Raman matrix-element

$$\langle \psi_{s2} | H_R^{(DM)} | \varphi, B^x \rangle \sim \sin\alpha \sim B^x M \ .$$

The $23.2\,\mathrm{cm}^{-1}$-mode would therefore be observable only in the ordered phase and in an external magnetic field, consistent with experiment. Having identified this mode with the transition to ψ_{s2} we have then that

$$\Delta E_{s2} = 2J_1 - 2J_2 = \nu_{sing} \sim 33\,\mathrm{K} \ . \qquad (13)$$

Considering (13) and the magnetic susceptibility [6,7] for $T > T_N$ we find a good fit with $J_1 \sim 47\,\mathrm{K}$ and $J_2 \sim 31\,\mathrm{K}$ which yields $J_2/J_1 \sim 0.66$. The experimental transition temperature [7] of $T_N^{(\mathrm{Br})} = 11.4$ K for $Cu_2Te_2O_5Br_2$ implies via the self-consistency condition (6) that $J_c \sim 0.85 J_1$.

Moreover, recalling Eqs. (7) and (10), for $B_x = 6\,\mathrm{T}$ the energy ΔE_{s2} of the excited singlet shifts by about $0.12\,\mathrm{cm}^{-1}$. This increase is too small to be resolved by Raman, although the data presented in inset b) of Fig. 5 seem to indicate a small increase.

Longitudinal magnon.- We observe that the mean-field Hamiltonian (3) leads to a $\mathbf{Q} = \mathbf{0}$ ordering for $J_c > 0$ and the soft longitudinal magnon $|\tilde{\varphi}\rangle$ should be directly observable with Raman. For $J_c < 0$ ordering with $\mathbf{Q} = \pi$ would occur and additional backfolding to the zone-center via residual lattice distortions would be necessary. The matrix-element $\langle \tilde{\varphi} | H_R | \varphi \rangle$ of the Raman-operator $H_R \sim \mathbf{S}_i \cdot \mathbf{S}_j$ $(i,j = 1,\ldots,4)$ is $\sim \cos\varphi \sin\varphi$. It vanishes in the decoupled-tetrahedra limit $J_c = 0$, $\varphi = 0$ and the transition should be observable only in the ordered phase.

Summarizing, the Raman mode at ν_{long} =16.3 cm^{-1} = 23.4 K in Fig. 5 (i) has been shown [7] to become soft at the ordering temperature, (ii) it is observable only in the condensed phase and its energy increases quadratically (compare Eq. (11)) with the field. We interpret it therefore as a longitudinal magnon.

The energy of this mode is strongly suppressed below its mean-field energy $E_{\tilde{\varphi}} - E_{\varphi} = 54\,\mathrm{K}$ by dispersion. We can estimate the magnitude of this suppression by comparison with the results of a bond-operator-theory for a coupled dimer system [15,16] (alternatively one may use a generalized RPA-approach [17]). The effective dimer-states are $(\psi_{s1}, \psi_{t1}^{\alpha})$. The gap of the longitudinal magnon has the form [15]

$$\Delta_{\mathrm{long}} = \Delta_{\mathrm{max}} \sqrt{1 - \left(J_c^{(qc)}/J_c \right)^2} \ . \qquad (14)$$

For $Cu_2Te_2O_5Br_2$ we have $J_c = 0.85 J_1$ $((J_c^{(qc)}/J_c)^2 = 0.78)$ and $\Delta_{\mathrm{long}} \approx 0.47 \Delta_{\mathrm{max}}$. The energy scale Δ_{max} occuring in Eq. (14) is set by the longitudinal magnon-gap in the classical Néel ordered state, i.e. in the limit of strong inter-dimer (tetrahedra) couplings, where it has the value $\Delta_{\mathrm{max}} \to J_c$. With $J_c \approx 0.85 J_1$ and $J_1 \approx 47\,\mathrm{K}$ we then find for $Cu_2Te_2O_5Br_2$ that $\Delta_{\mathrm{long}} \approx 19\,\mathrm{K}$, which is qualitatively in agreement with the experimental value $\Delta_{\mathrm{long}}^{(\mathrm{exp})} = \nu_{long} = 23.4\,\mathrm{K}$, see the inset Fig. 5 b. Due to the renormalization of Δ_{long} by the fluctuations near the quantum-critical point, see Eq. (14), we cannot easily quantitatively estimate its dependence on an external magnetic field, as presented in inset b) of Fig. 5.

Comparison with $Cu_2Te_2O_5Cl_2$.- The magnitude of the intra-tetrahedral parameters have been estimated [6] from susceptibility measurements to be similar both for $Cu_2Te_2O_5Br_2$ and the isostructural $Cu_2Te_2O_5Cl_2$. The substantially enhanced Néel temperature [7] of $T_N^{(\mathrm{Cl})} =$ 18.2 K indicates a larger inter-dimer coupling for the Cl-compound. This notion is consistent with the Raman-results for doped compounds which indicates a harding of the excitations with Cl-content, as predicted by Eq. (14) [12]. We did not attempt a quantitative analysis of the coupling parameters for $Cu_2Te_2O_5Cl_2$ since we were not able to observe the second singlet as in $Cu_2Te_2O_5Br_2$. Indeed, a generalized tight-binding analysis of band-structure calculations [18] indicates that the ratio of the intra-dimer couplings J_2/J_1 in $Cu_2Te_2O_5Cl_2$ is smaller than in $Cu_2Te_2O_5Br_2$. These findings also suggest that for $Cu_2Te_2O_5Cl_2$ the excited singlet with energy $E_{s2} = 2J_1 - 2J_2$ should probably be located in the energy-range of the magnetic continuum and thus not observable separately.

Conclusions.- We have presented a comprehensive set of theory and experimental data indicating that the isostructural spin-tetrahedral compounds $Cu_2Te_2O_5(Br_xCl_{1-x})_2$ constitute a series of systems with a systematic variation of the microscopic parameters with respect to a quantum critical transition. We have pointed out the importance of the low-lying singlet for the magnetic state and reported the observation of a low-energy longitudinal magnon.

We acknowledge the support of the German Science Foundation (DFG SP1073, SFB484), and important discussions with Wolfram Brenig, Frederic Mila, Jens Jensen and T. Saha-Dasgupta.

[1] I. Affleck and G.F. Wellman, Phys. Rev B **46**, 8934 (1992). H.J. Schulz, Phys. Rev. Lett. **77**, 2790 (1996). F.H.L. Essler, A.M. Tsvelik, and G. Delfino, Phys. Rev. B **56**, 11001 (1997).

[2] B. Lake, D.A. Tennant and S.E. Nagler, Phys. Rev. Lett. **85**, 832 (2000).
[3] A. Zheludev *et al.*, Phys. Rev. B **65**, 014402 (2002).
[4] S. Raymond *et al.* Phys. Rev. Lett. **82**, 2382 (1999).
[5] M. Enderle *et al.*, Phys. Rev. B **59**, 4235 (1999).
[6] M. Johnsson, K.W. Törnroos, F. Mila and P. Millet, Chem. Mater. **12**, 2853 (2000).
[7] P. Lemmens *et al.*, Phys. Rev. Lett. **87**, 227201 (2001).
[8] W. Brenig and K.W. Becker, Phys. Rev. B **64**, 214413 (2001).
[9] K. Totsuka and H-J. Mikeska, to be published in Phys. Rev. **B** (2002), cond-mat/0207176.
[10] Other possible ordering patterns, like $\langle S_1^z + S_2^z + S_3^z + S_4^z \rangle$, lead to first-order phase transitions.
[11] For $J_c/J_1 \to \infty$ the coupling to the quintuplet ψ_q neglected in Eq. (8) would contribute and the zero-T moment would take the mean-field value of 1/2.
[12] P. Lemmens *et al.*, Journ. Phys. Chem. Solids **63/6-8**, (2002) 1115.
[13] Note that there is a smaller decreasing contribution in B_x to the Néel temperature coming from the log-term in Eq. (7) due to an enhancement of the effective J_1.
[14] I.J. Dzyaloshinskii, J. Phys. Chem. Solids **4**, 241 (1958). T. Moriya, Phys. Rev **120**, 91 (1960).
[15] T. Sommer, M. Vojta and K.W. Becker, Euro. Phys. J. B **23**, 329 (2001).
[16] B. Normand and T.M. Rice, Phys. Rev. B **56**, 8760 (1997).
[17] J. Jensen and A.R. Mackintosh, *"Rare Earth Magnetism: Structures and Excitations"*, Oxford University Press, Oxford (1991).
[18] R. Valentí, T. Saha-Dasgupta, C. Gros, and H. Rosner cond-mat/0301119

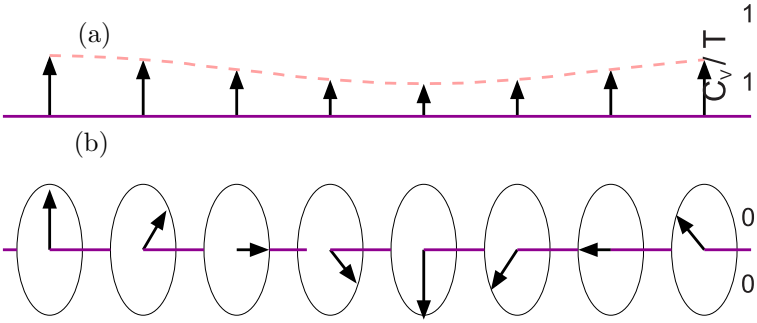

FIG. 1. Schematic representation of (a) a longitudinal magnon (b) a transversal magnon.

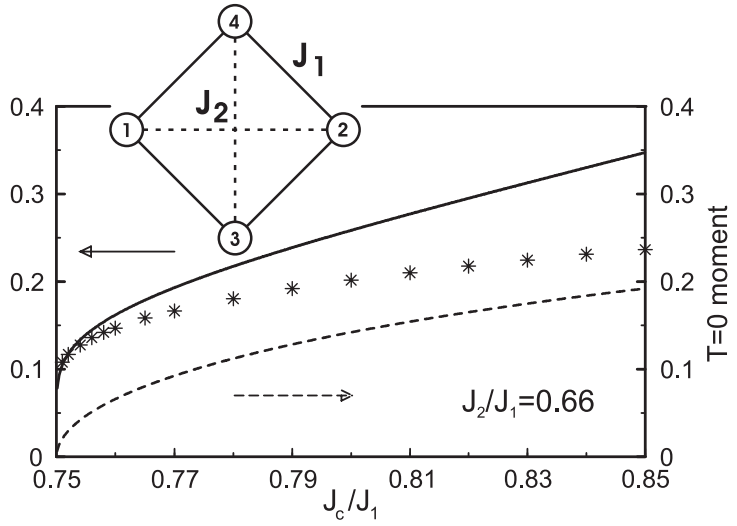

FIG. 2. Neél-temperature (left scale) and spin tetrahedra mean-field moment (right scale) for $J_2/J_1 = 0.66$. Shown is the analytic approximation to leading order by Eq. (7) (solid line) and the numerical solution of the self-consistency equation (6) (stars). The dashed line (right scale) is the magnetic moment at zero-temperature Eq. (8). Note the logarithmic singularity in T_N for $J_c \to 0.75 J_1$. Inset: Cu tetrahedron with exchange couplings J_1 and J_2 (solid/dashed lines).

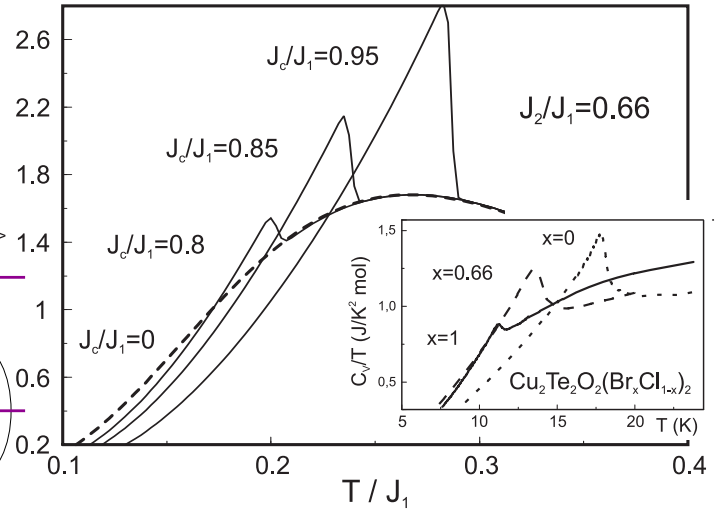

FIG. 3. Mean-field results for the specific heat of spin tetrahedra coupled by J_c. The inset shows the specific heat of $Cu_2Te_2O_5(Br_xCl_{1-x})_2$ with x=1, 0.66 and 0. The data with x=0 and 1 are compiled from [7].

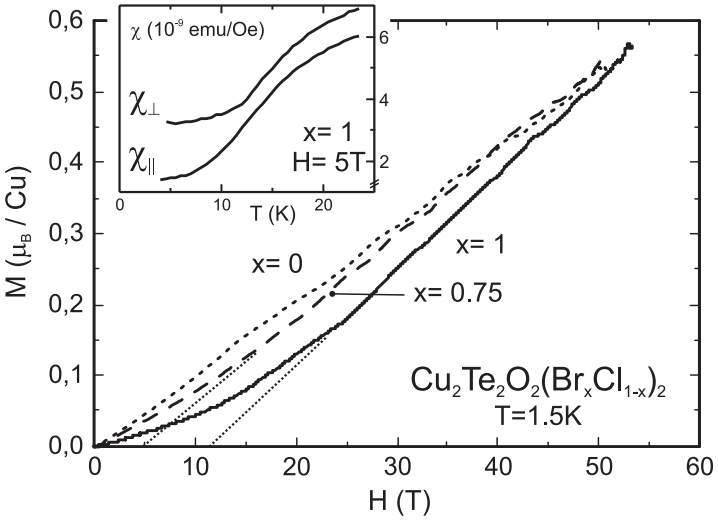

FIG. 4. High-field magnetization of $Cu_2Te_2O_5(Br_xCl_{1-x})_2$ powder samples for x=1, 0.75 and 0. The data with x=0.66 is omitted here for clarity. Dotted lines correspond to high field extrapolations. The inset shows the anisotropic magnetic susceptibility of $Cu_2Te_2O_5Br_2$ single crystals.

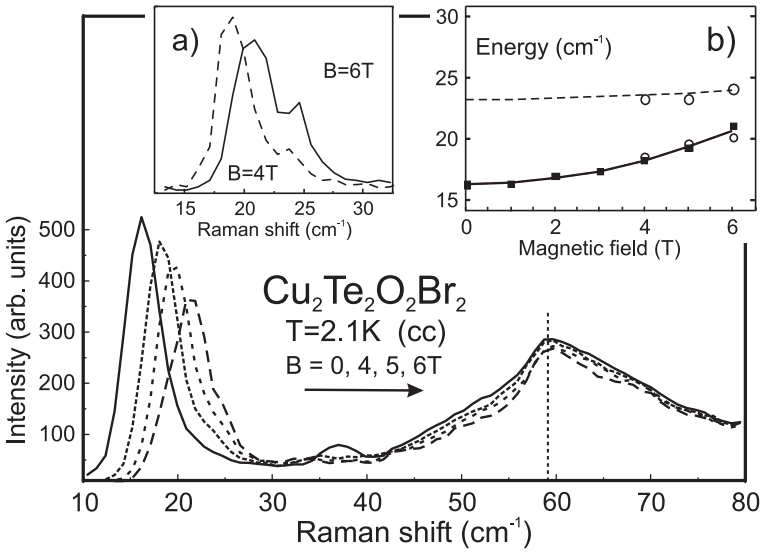

FIG. 5. Raman spectra of $Cu_2Te_2O_5Br_2$ in a magnetic field. The insets show a) spectra with higher resolution and b) the shift of the $\nu_{sing} = 23.2\,\mathrm{cm}^{-1}$ mode (upper open symbols) and the $\nu_{long} = 16.3\,\mathrm{cm}^{-1}$ mode (lower full and open symbols) as a function of the magnetic field. The dashed line shows the field dependence of the transition temperature [7] and the full line is a fit to the data proportional to the square of the magnetic field. The open (full) symbols show data with high resolution (normal resolution).